Automatica 45 (2009) 10–24

Contents lists available at ScienceDirect

Automatica

journal homepage: www.elsevier.com/locate/automatica

An adaptive freeway traffic state estimator☆

Yibing Wang [a,*], Markos Papageorgiou [b,1], Albert Messmer [c,2], Pierluigi Coppola [d,3], Athina Tzimitsi [b,1], Agostino Nuzzolo [d,3]

[a] Institute of Transport Studies, Department of Civil Engineering, Monash University, VIC 3800, Australia

[b] Dynamic Systems and Simulation Laboratory, Department of Production Engineering and Management, Technical University of Crete, 73100 Chania, Greece

[c] Groebenseeweg 2, D-82402, Seeshaupt, Germany

[d] Department of Civil Engineering, "Tor Vergata" University of Rome, Rome, Italy

ARTICLE INFO

Article history:
Received 6 May 2006
Received in revised form
7 November 2007
Accepted 4 May 2008
Available online 18 November 2008

Keywords:
Stochastic macroscopic traffic flow model
Extended Kalman filter
Freeway traffic state estimation
Joint state and parameter estimation
Congestion
Weather conditions
Traffic incidents
Detector faults
Traffic incident alarm
Detector fault alarm

ABSTRACT

Real-data testing results of a real-time nonlinear freeway traffic state estimator are presented with a particular focus on its adaptive features. The pursued general approach to the real-time adaptive estimation of complete traffic state in freeway stretches or networks is based on stochastic nonlinear macroscopic traffic flow modeling and extended Kalman filtering. One major innovative aspect of the estimator is the real-time joint estimation of traffic flow variables (flows, mean speeds, and densities) and some important model parameters (free speed, critical density, and capacity), which leads to four significant features of the traffic state estimator: (i) avoidance of prior model calibration; (ii) automatic adaptation to changing external conditions (e.g. weather and lighting conditions, traffic composition, control measures); (iii) enabling of incident alarms; (iv) enabling of detector fault alarms. The purpose of the reported real-data testing is, first, to demonstrate feature (i) by investigating some basic properties of the estimator and, second, to explore some adaptive capabilities of the estimator that enable features (ii)–(iv). The achieved testing results are quite satisfactory and promising for further work and field applications.

1. Introduction

Real-time freeway **traffic state estimation** refers to estimating **traffic flow variables** (flows, space mean speeds, and densities) for a considered freeway stretch (see e.g. Wang and Papageorgiou (2005), Wang, Papageorgiou, and Messmer (2007)) or freeway network (Wang, Papageorgiou, & Messmer, 2006; Wang et al., in press) with an adequate time resolution (e.g. 5–10 s) and spatial resolution (e.g. 500 m or less) based on a limited amount of available measurement data from traffic detectors of various types (e.g. inductive loops, video cameras, radar senors). It should be emphasized that the number of traffic flow variables to be estimated may be much larger than the number of traffic flow variables that are directly measured, and this is in fact the essential contribution of the traffic state estimation task. Real-time freeway traffic state estimation is a fundamental task for freeway traffic surveillance and control (Papamichail, Papageorgiou, & Wang, 2007) and has attracted a lot of investigation efforts in the past three decades. Related research proposed traffic state estimation algorithms that were almost exclusively based on macroscopic traffic flow modeling and (extended) Kalman filtering; see a concise review in Wang and Papageorgiou (2005). Following a similar avenue, this topic was recently investigated further, and a general approach to the design of freeway traffic state estimators was proposed (Wang & Papageorgiou, 2005). One distinct innovative aspect of this recent work is **on-line model parameter estimation** (Wang & Papageorgiou, 2005; Wang, Papageorgiou, & Messmer, 2003; 2006), i.e. real-time **joint estimation** of all involved traffic flow variables and some important parameters (free speed, critical density, capacity) of the macroscopic traffic flow model employed by the traffic state

☆ This paper was not presented at any IFAC meeting. This paper was recommended for publication in revised form by Associate Editor Keum-Shik Hong under the direction of Editor Mituhiko Araki.

* Corresponding author. Tel.: +61 3 9905 9339; fax: +61 3 9905 4944.
E-mail addresses: yibing.wang@eng.monash.edu.au (Y. Wang), markos@dssl.tuc.gr (M. Papageorgiou), Albert.Messmer@t-online.de (A. Messmer), coppola@ing.uniroma2.it (P. Coppola), tzimitsi@gmail.com (A. Tzimitsi), nuzzolo@ing.uniroma2.it (A. Nuzzolo).

1 Tel.: +30 28210 37289; fax: +30 28210 37584.

2 Tel.: +49 8801 95101; fax: +49 8801 95102.

3 Tel.: +39 06 72597059; fax: +39 06 72597005.

0005-1098/$ – see front matter © 2008 Elsevier Ltd. All rights reserved.
doi:10.1016/j.automatica.2008.05.019

estimator. With the on-line model parameter estimation, four significant features may be achieved for the traffic state estimator:

(i) *Avoidance of off-line model calibration*: When applying macroscopic traffic flow modeling to a specific freeway stretch or network, appropriate model parameter values are needed, which are usually not precisely known beforehand and may indeed be different from site to site. Therefore, before a traffic state estimator can be applied to a specific site, a tedious model calibration procedure usually has to be conducted off-line based on available traffic measurement data to identify the corresponding values of the model parameters (see e.g. Cremer and Papageorgiou (1981) and Papageorgiou, Blosseville, and Haj-Salem (1990)). However, if the model parameter values can also be properly estimated on-line (i.e. estimated simultaneously with the interested traffic flow variables), the extra workload for off-line model calibration may be avoided.

(ii) *Automatic adaptation to changing external conditions*: For a given site, the model parameter values may have to be changed significantly in real-time, in order for the employed model to reflect the impact of changing external conditions (weather and lighting conditions, percentage of trucks, variable speed limits applied, etc.) on the traffic flow characteristics. With fixed model parameter values (even if carefully pre-identified), a traffic state estimator may not be able to work well under strongly changing external conditions. However, if the estimator can adapt its model to the external condition changes via on-line model parameter estimation using real-time traffic measurements, the corresponding traffic situations may still be handled appropriately.

(iii) *Enabling of incident alarms*: In case of incidents, the traffic flow characteristics along the concerned freeway stretch may change substantially; this may also be reflected in correspondingly drastic changes of some model parameter values. With on-line model parameter estimation, such abrupt changes may be identified in real time, and hence the incident occurrence may be recognized promptly, leading to corresponding incident alarms for traffic operators.

(iv) *Enabling of detector fault alarms*: In case of strong detector malfunctions, the estimator has to adjust its model parameters radically in order for the local traffic state estimates to approach the disfigured measurements. Hence, the on-line model parameter estimates may also be used as an indicator for serious detector malfunction.

Recently a freeway traffic state estimator using on-line model parameter estimation was developed and successfully tested in simulation (Wang & Papageorgiou, 2005; Wang et al., 2006), whereby the significance of on-line model parameter estimation for proper traffic state estimation as well as the aforementioned estimator features were preliminarily demonstrated. In order to draw more reliable conclusions, the same traffic state estimator was also tested using real traffic measurement data collected from the A92 Freeway close to Munich, Germany, and the A3 Freeway in South Italy. Some representative testing results are presented in this paper. It is important to mention that the average inter-detector spacing used in these recent tests is much larger than that reported in most previous works (see Wang and Papageorgiou (2005) for a review therein).

The next section presents a stochastic nonlinear macroscopic traffic flow model and a simple traffic measurement model, based on which the traffic state estimator is designed with the extended Kalman filtering. The A92 real-data testing in Germany is subsequently reported so as, first, to demonstrate feature (i) by investigating some basic properties of the estimator and, second, to explore some adaptive capabilities of the estimator that enable features (ii) and (iii), particularly under changing external conditions and non-recurrent traffic incidents. The A3 real-data testing in south Italy provides a large-scale field application example for the designed traffic state estimator, which demonstrates feature (iv) as well as the overall adaptive capabilities of the estimator. The main conclusions along with some additional remarks on state estimation of nonlinear systems corrupted with noise are provided in a final section.

2. Modeling and methodology

2.1. Stochastic macroscopic traffic flow model

A stochastic version of a nonlinear second-order validated macroscopic traffic flow model (Papageorgiou et al., 1990) is employed in this paper to describe the dynamic behavior of traffic flow along a freeway stretch in terms of appropriate aggregated traffic flow variables. Any considered freeway stretch is subdivided into a number N of segments with lengths $\Delta_i, i = 1, \ldots, N$, while the time is discretized based on a time step T and the time index $k = 0, 1, 2, \ldots$. The aggregated traffic flow variables are defined in this discrete space–time frame as follows:

- Traffic density $\rho_i(k)$ (in veh/km/lane) is the number of vehicles in segment i at time instant kT, divided successively by the segment length Δ_i and lane number λ_i.
- Space mean speed $v_i(k)$ (in km/h) is the average speed of all vehicles included in segment i at time instant kT.
- Traffic flow $q_i(k)$ (in veh/h) is the number of vehicles leaving segment i during the time period $[kT, (k+1)T]$, divided by T.
- On-ramp inflow $r_i(k)$ and off-ramp outflow $s_i(k)$ (both in veh/h) at the segment i (if any).

It is shown in Papageorgiou et al. (1990) that the macroscopic model works pretty accurately with segment lengths Δ_i in the order of 500 m (or less) and model time step T in the order of 10 s. Note that, for numerical stability reasons, T and Δ_i must be chosen such that $T < \Delta_i/v_f$, where v_f denotes the free speed (to be explained in what follows). While subdividing a freeway stretch into segments, care should be taken that all geometric inhomogeneities or installed traffic detectors along the freeway stretch are located at the boundaries of the segments. Moreover, each segment is allowed to have at most one on-ramp or one off-ramp, preferably at the upstream boundary of the segment.

For a segment i, the stochastic nonlinear difference equations of the model are as follows:

$$\rho_i(k+1) = \rho_i(k) + \frac{T}{\Delta_i \lambda_i}[q_{i-1}(k) - q_i(k) + r_i(k) - s_i(k)] \tag{1}$$

$$s_i(k) = \beta_i(k) \cdot q_{i-1}(k) \tag{2}$$

$$\begin{aligned} v_i(k+1) = {} & v_i(k) + \frac{T}{\tau}[V(\rho_i(k)) - v_i(k)] \\ & + \frac{T}{\Delta_i} v_i(k)[v_{i-1}(k) - v_i(k)] \\ & - \frac{\nu T}{\tau \Delta_i} \frac{[\rho_{i+1}(k) - \rho_i(k)]}{\rho_i(k) + \kappa} - \frac{\delta T}{\Delta_i \lambda_i} \frac{r_i(k) v_i(k)}{\rho_i(k) + \kappa} + \xi_i^v(k), \end{aligned} \tag{3}$$

$$V(\rho) = v_f \exp\left[-\frac{1}{a}\left(\frac{\rho}{\rho_{cr}}\right)^a\right] \tag{4}$$

$$q_i(k) = \rho_i(k) \cdot v_i(k) \cdot \lambda_i + \xi_i^q(k) \tag{5}$$

where (1), (3)–(5) are the conservation equation, dynamic speed equation, stationary speed equation, and transport equation, respectively; $\beta_i(k)$ (dimensionless) denotes the exiting rate at the off-ramp in segment i (if any); τ, ν, κ, δ, v_f, ρ_{cr}, and a are model parameters that may be given the same values for all segments of the considered freeway stretch; $\xi_i^v(k)$ and $\xi_i^q(k)$ denote zero-mean white noise acting on the empirical speed equation and the approximate flow equation, respectively, to reflect the modeling

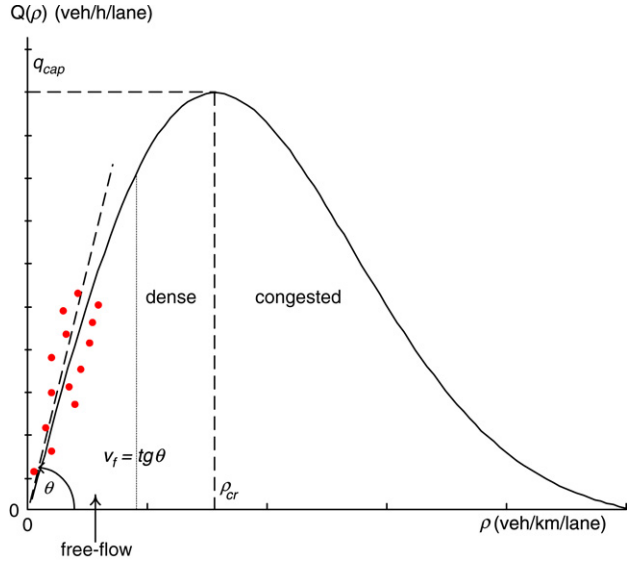

Fig. 1. Fundamental diagram and related parameters (free speed v_f, critical density ρ_{cr}, and capacity q_{cap}).

inaccuracies. Their variances may be set in accordance with the related equation accuracy that is known from the previous off-line model validation exercises (Cremer & Papageorgiou, 1981; Papageorgiou et al., 1990). Note that (1) is not corrupted by noise as it describes the conservation of vehicles, which holds strictly in any case.

From (4), the fundamental diagram expressing a stationary flow–density relationship that is well known in traffic engineering, can be derived as

$$Q(\rho) = \rho \cdot V(\rho) = \rho \cdot v_f \exp\left[-\frac{1}{a}\left(\frac{\rho}{\rho_{cr}}\right)^a\right] \tag{6}$$

based on which the (flow) capacity of a stretch (per lane) may be deduced as

$$q_{cap}(v_f, \rho_{cr}, a) = v_f \cdot \rho_{cr} \cdot \exp[-1/a]. \tag{7}$$

Fig. 1 plots the nonlinear bell-shaped fundamental diagram (6) that is characterized by the free speed (or free-flow speed) v_f, critical density ρ_{cr}, and capacity q_{cap}. More specifically, v_f is the mean driving speed when any driver is not impeded/influenced by other vehicles on the freeway; its value corresponds to the slope of the $Q(\rho)$-curve at $\rho = 0$; q_{cap} is the maximum attainable flow (per lane), while ρ_{cr} is the traffic density at which the traffic flow reaches q_{cap}. Albeit not depicted in Fig. 1, the exponent a determines the capacity (given the free speed and critical density) and influences the shape of the fundamental diagram especially at the right of the critical density.

The values of τ, ν, κ, δ, v_f, ρ_{cr}, and a are usually not precisely known beforehand and may be different from site to site; even for a given site, these parameter values may vary with environmental and further external conditions (weather and lighting conditions, percentage of trucks, variable speed limits applied, etc.).[4] However, the model results are known to be most sensitive to variations of the fundamental diagram parameters v_f, ρ_{cr}, and a (Papageorgiou et al., 1990). Therefore, this paper only considers v_f, ρ_{cr}, and a as unknown model parameters for on-line estimation, while the values of the other model parameters are set as determined by previous off-line model calibrations (Cremer & Papageorgiou, 1981; Papageorgiou et al., 1990).

For any segment i, $q_i(k)$ can be calculated from $\rho_i(k)$ and $v_i(k)$ via (5) and replaced in (1), hence $\rho_i(k)$ and $v_i(k)$ may be viewed as independent segment variables. On the other hand, for each time instant k, the traffic flow variables $q_{i-1}(k)$, $v_{i-1}(k)$ and $\rho_{i+1}(k)$ as well as $r_i(k)$ and $\beta_i(k)$ (if any) are needed for calculating $\rho_i(k+1)$ and $v_i(k+1)$. These variables are boundary variables of segment i, incorporating the impact of the adjacent segments on the traffic dynamics of segment i. If a freeway stretch is considered as a tandem connection of a number of segments, the complete macroscopic model for the whole stretch can be built upon a chain of segment models interconnected via some of their respective boundary variables. More precisely, with (2) and (5) substituted into (1) and (4) into (3), respectively, the stretch model of N segments consists of $2N$ model equations with $2N$ independent segment variables $\rho_1, v_1, \rho_2, v_2, \ldots, \rho_N, v_N$; three unknown model parameters v_f, ρ_{cr}, and a; and a number of boundary variables: (a) flow at the stretch origin q_0, (b) speed at the stretch origin v_0, (c) density at the stretch end ρ_{N+1}, (d) on-ramp inflows r_i (if any), and (e) off-ramp exiting rates β_i (if any).

This stretch model combined with a node model delivers a freeway network model, see Wang et al. (2006) for details.

2.2. Model of traffic measurements

Traffic detectors of various types (e.g. loops, cameras, radar sensors, etc.) are usually placed along freeway stretches at a separation of up to several kilometres as a main device for obtaining real-time traffic measurements. This paper only considers flow and mean speed measurements.

Consider a traffic detector installed at the boundary of segments i and $i+1$. For its flow measurement, we have

$$m_i^q(k) = q_i(k) + \gamma_i^q(k) \tag{8}$$

where $m_i^q(k)$ denotes the flow measurement during the time period $[kT, (k+1)T]$, and $\gamma_i^q(k)$ the flow measurement noise. Except for the measurement of q_0, we have by (5)

$$m_i^q(k) = \rho_i(k) \cdot v_i(k) \cdot \lambda_i + \xi_i^q(k) + \gamma_i^q(k). \tag{9}$$

For the mean speed measurement, we have

$$m_i^v(k) = v_i(k) + \gamma_i^v(k) \tag{10}$$

where $m_i^v(k)$ denotes the space mean speed that may be calculated as the harmonic mean of measured individual-vehicle speeds during the time period $[kT, (k+1)T]$ and $\gamma_i^v(k)$ the related speed measurement noise. For on-ramps and off-ramps, only flow measurements are of interest. The on-ramp and off-ramp flow measurements $m_i^r(k)$ and $m_i^s(k)$ (if any) are modeled, respectively, as

$$m_i^r(k) = r_i(k) + \gamma_i^r(k) \tag{11}$$

$$m_i^s(k) = s_i(k) + \gamma_i^s(k) = \beta_i(k) \cdot (\rho_{i-1}(k) \cdot v_{i-1}(k) \cdot \lambda_{i-1} + \xi_{i-1}^q(k)) + \gamma_i^s(k) \tag{12}$$

where $\gamma_i^r(k)$ and $\gamma_i^s(k)$ denote the on-ramp and off-ramp flow measurement noise, respectively. All measurement noise involved in (8)–(12) is assumed zero-mean white. The standard deviation of each measurement noise is assumed known and should reflect the reliability level of the corresponding measurements. The utilized covariance of the measurement noise can be found in Wang and Papageorgiou (2005) and Wang et al. (2007).

[4] For instance, the effect of various weather conditions on the free speed is reported in Kyte, Khatib, Shannon, and Kitchener (2001), while the impact of variable speed limits on aggregate traffic flow behavior has recently been reported in Papageorgiou, Kosmatopoulos, and Papamichail (2008).

2.3. State-space model and estimator design

For any freeway stretch, let vectors $\mathbf{z}$, $\mathbf{d}$, $\mathbf{p}$, and $\boldsymbol{\xi}_1$ include, respectively, all segment variables, stretch boundary variables, unknown model parameters, and modeling noise. Then the macroscopic traffic flow model of a freeway stretch can be expressed in a compact state-space form:

$$\mathbf{z}(k+1) = \mathbf{h}[\mathbf{z}(k), \mathbf{d}(k), \mathbf{p}(k), \boldsymbol{\xi}_1(k)] \tag{13}$$

where $\mathbf{h}$ is a nonlinear differential vector function corresponding to the $2N$ model equations previously mentioned. The utilization of (13) requires the real-time availability of $\mathbf{d}(k)$ and (real-time) determination of $\mathbf{p}(k)$. However, some elements of $\mathbf{d}(k)$ may not be measured or even not measurable (Wang & Papageorgiou, 2005; Wang et al., 2006), while $\mathbf{p}(k)$ is normally unknown (or partially unknown). In order to overcome the obstacle of partially missing boundary measurements and unknown model parameters, model (13) may be extended using two random-walk equations:

$$\mathbf{d}(k+1) = \mathbf{d}(k) + \boldsymbol{\xi}_2(k) \tag{14}$$

$$\mathbf{p}(k+1) = \mathbf{p}(k) + \boldsymbol{\xi}_3(k) \tag{15}$$

where $\boldsymbol{\xi}_2(k)$ and $\boldsymbol{\xi}_3(k)$ are vectors of zero-mean white noise, whose covariance matrices must be chosen so as to reflect typical time variations of the boundary variables and model parameters.

The combination of (13)–(15) leads to the following augmented state-space model

$$\mathbf{x}(k+1) = \mathbf{f}[\mathbf{x}(k), \boldsymbol{\xi}(k)], \tag{16}$$

where $\mathbf{x} = \left[\mathbf{z}^{\mathrm{T}}\ \mathbf{d}^{\mathrm{T}}\ \mathbf{p}^{\mathrm{T}}\right]^{\mathrm{T}}$, $\boldsymbol{\xi} = \left[\boldsymbol{\xi}_1^{\mathrm{T}}\ \boldsymbol{\xi}_2^{\mathrm{T}}\ \boldsymbol{\xi}_3^{\mathrm{T}}\right]^{\mathrm{T}}$; the nonlinear differentiable vector function $\mathbf{f}$ can be determined accordingly. In this paper, vector $\mathbf{x}$ is referred to as the **traffic state**.

Consider a freeway stretch with traffic detectors installed at its uppermost and lowermost boundaries, at some on/off-ramps, and perhaps also at some stretch-internal locations. The measurement model (8)–(12) can be written in a compact form as well:

$$\mathbf{y}(k) = \mathbf{g}[\mathbf{x}(k), \boldsymbol{\eta}(k)] \tag{17}$$

where the output vector $\mathbf{y}$ consists of all available measurements of flow and mean speed; $\mathbf{g}$ is a nonlinear differentiable vector function; vector $\boldsymbol{\eta}$ is a function of state noise vector $\boldsymbol{\xi}$ and measurement noise vector $\boldsymbol{\gamma}$. Eqs. (16) and (17) constitute a complete freeway traffic dynamic system $\boldsymbol{\Sigma}(\mathbf{x}, \mathbf{y}, \boldsymbol{\xi}, \boldsymbol{\eta})$.

Given real-time measurements $\mathbf{y}(k)$, the traffic state estimator designed for $\boldsymbol{\Sigma}(\mathbf{x}, \mathbf{y}, \boldsymbol{\xi}, \boldsymbol{\eta})$ delivers state estimates:

$$\hat{\mathbf{x}}(k+1/k) = \mathbf{f}[\hat{\mathbf{x}}(k/k-1), 0] + \mathbf{K}(k)[\mathbf{y}(k) - \mathbf{g}(\hat{\mathbf{x}}(k/k-1), 0)].$$

Although some canonical forms other than $\boldsymbol{\Sigma}(\mathbf{x}, \mathbf{y}, \boldsymbol{\xi}, \boldsymbol{\eta})$ can also be constructed based on the presented traffic flow model and measurement model, $\boldsymbol{\Sigma}(\mathbf{x}, \mathbf{y}, \boldsymbol{\xi}, \boldsymbol{\eta})$ leads to a straightforward, general, and unique formulation of the traffic state estimator for any freeway stretch or network of any topology, size, and characteristics, with any suitable detector configuration (Wang & Papageorgiou, 2005; Wang et al., 2006).

3. Performance evaluation using real measurement data

3.1. A normal congestion case

The first test of the designed traffic state estimator was conducted with real traffic measurement data collected from a 2-lane westbound stretch of the A92 Freeway close to Munich, Germany, which is within A92's most congested part between the Munich airport and the junction AK Neufahrn. As shown in Fig. 2a, the test stretch has an on-ramp at its beginning while four loop detector stations (gray bars) are installed along the stretch.

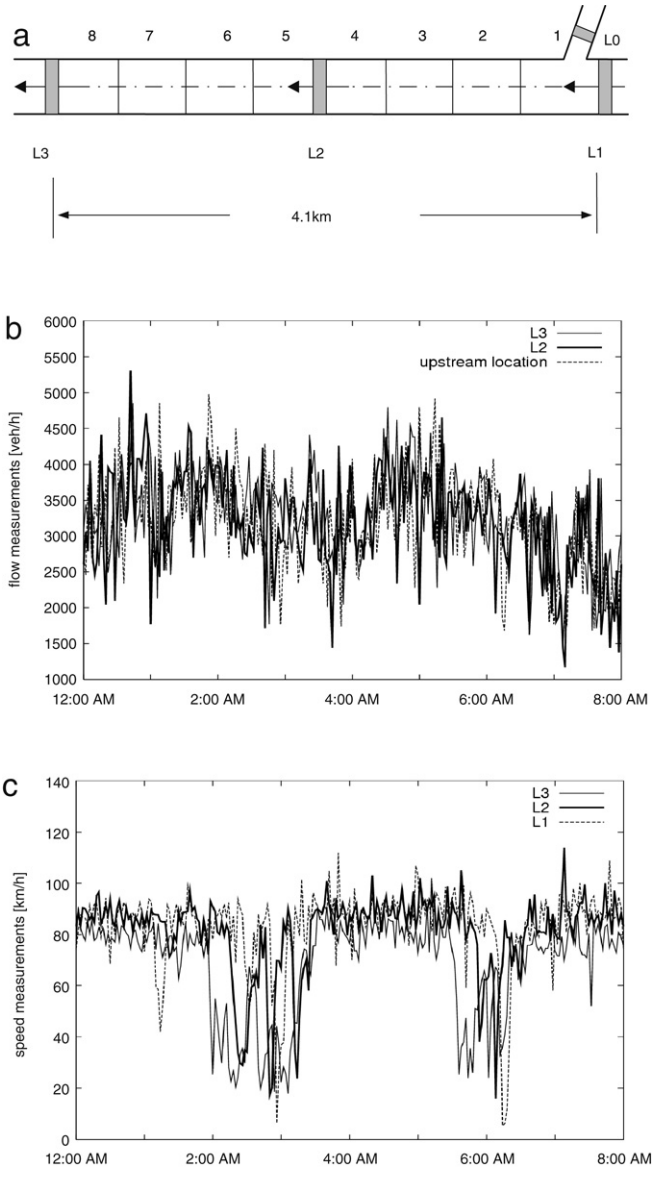

Fig. 2. Test stretch 1 in A92 freeway close to Munich: (a) stretch layout and detector configuration; (b) flow measurements; (c) mean speed measurements.

The single-car data recorded by the detectors were converted into aggregated traffic measurements of flow and space mean speed every minute. The utilized flow and speed measurements of 8 h were collected on March 30, 2001. Fig. 2b displays the flow measurements, with the plotted upstream flow being the summation of the flow measurements at L0 and L1 (the flow at L0 is around 10% of that at L1). Fig. 2c displays the speed measurements at L1, L2, and L3. Two distinguished oscillatory (stop-and-go) speed drops are observed at each mainstream measurement location, during which the corresponding flows are noticeably reduced. Moreover, the flow measurements keep reducing on average after 6:00 PM due to the decreasing traffic demand. As illustrated in Fig. 2a, the test stretch is subdivided into 8 segments, each with an approximate length of 500 m. Accordingly, the time step T of the estimator model is set equal to 10 s. The free speed, critical density, and capacity are assumed to be the same for the whole stretch. The flow and speed measurements from L0, L1, and L3 were used to feed the estimator, while the flow and speed measurements from L2 were only used to compare with the flow and speed estimates of segment 4 so as to evaluate the performance of the estimator.

The standard deviation (SD) values were set to be 100 veh/h and 10 km/h for the flow and speed modeling noise, respectively, and the same SD values were also used for the flow and speed measurement noise. In fact, the SD values of the modeling noise were chosen so as to reflect the expected accuracy level of the model equations (Cremer & Papageorgiou, 1981; Papageorgiou et al., 1990), while the SD values of the measurement noise were specified according to the levels of typical measurement error of loop detectors. Note that the SD values may need to be slightly tuned for specific sites. For all test examples reported in this paper, the utilized SD values vary between 50 and 200 veh/h for flows and between 5 and 10 km/h for speeds, and were always set constant for a given site.

The estimator's performance was first examined without using on-line model parameter estimation (i.e. keeping the parameters constant at some pre-specified values over the investigation time horizon). To this end, three groups of parameter values were considered, namely (95, 30, 2042), (85, 25, 1289), and (100, 50, 3894), each for the free speed (km/h), critical density (veh/km/lane), and capacity (veh/h/lane). These parameter groups are referred to as parameter conditions 1, 2, and 3, respectively. The estimator was found capable of tracking the speed drops only under parameter condition 1 as Fig. 3a presents, while the flow estimation was good under parameter conditions 1 and 3 (Fig. 3b). This demonstrates that:

(i) For a given test example, there exists (at least) one group of nominal model parameter values, with which pretty accurate traffic state estimates can be delivered by the estimator. Normally this specific group of parameter values can be obtained via off-line parameter identification.
(ii) If such nominal model parameter values are not well identified (e.g. as in the case of parameter conditions 2 and 3), then unacceptable traffic state estimation bias may result (even under free-flow conditions).

Next, the estimator is evaluated using on-line model parameter estimation, and the same parameter conditions 1–3 are used as initial conditions. Note that the model parameters actually estimated are v_f, ρ_{cr}, and a; however, since the flow capacity q_{cap} can be calculated with v_f, ρ_{cr}, and a through (7) and has a more apparent physical interpretation than the exponent a, we will present in the rest of the paper the estimates of v_f, ρ_{cr}, and q_{cap}. In order to check the dynamic evolution of the traffic state estimates as well as the stability of the estimator, the testing was conducted over a quadruple time horizon, whereby the traffic scenario of the first time horizon (12:00 AM–8:00 PM) was duplicated to the next three. Although the estimates of the free speed, critical density, and capacity converge at the end of the second time horizon (see e.g. Fig. 3c for the capacity estimation), satisfactory speed estimates at L2 are delivered under each initial condition already at the start of the second time horizon (Fig. 3d and e), while satisfactory flow estimates at L2 are obtained even from the start of the first time horizon (Fig. 3f). It is important to mention that the shown "slow" convergence under initial conditions 2 and 3, and hence the use of triple duplicate of the 8 h real data, are due to the "cold" start of the estimator, i.e. by use of an arbitrary initial matrix of the estimation covariance and by use of the initial model parameter values that were set unrealistically far from normal values (just to demonstrate the estimator's adaptive capability in achieving convergence even with these extreme initial values). In contrast, under normal operation conditions (i.e. with a "warm" start incorporating some prior field knowledge of the model parameters), the estimator is seen, in the subsequent sections with several demonstration examples (snowstorm, incident, and detector fault), to adapt the model parameters promptly as appropriate. In fact, even for the current test example with the "cold" start, the use of larger SD values for the model parameter noise $\boldsymbol{\xi}_3$ in (15) leads to faster convergence in the estimation of both traffic flow variables and model parameters.

In fact, a lower/higher SD of the noise for an estimated model parameter is a "message" to the extended Kalman filter that this parameter is less/more time-variant. More specifically, higher SDs are expected to lead to faster convergence of the parameter estimates but also more nervous behavior of the parameter estimates. The group of the SD values for $\xi^{v_f}(k)$, $\xi^{\rho_{cr}}(k)$, and $\xi^{a}(k)$ (see (15)) utilized for the results in Fig. 3c–f is (0.1 veh/h, 0.02 veh/km/lane, 0.002), while two more groups of SD values (0.2 veh/h, 0.04 veh/km/lane, 0.004) and (0.5 veh/h, 0.1 veh/km/lane, 0.01) were also considered for a sensitivity investigation; these three groups of the SD values are referred to as SD 1, 2, and 3. The test demonstrates that the estimates of traffic flow variables are little sensitive to the various groups of the SD values (see e.g. Fig. 3g for the speed estimates at L2), although the corresponding parameter estimation trajectories may be different (see e.g. Fig. 3h for the capacity estimates). Note that the speed estimates in Fig. 3g are actually obtained over the third time horizon under initial condition 2 (compare Fig. 3d, e, g), while virtually the same results as presented in Fig. 3g can be delivered from the start of the third time horizon onwards under any initial condition (due to the aforementioned convergence). This low sensitivity property of the estimator with regard to various SD values used guarantees to a large extent the robustness of the estimator and a very limited need for fine-tuning of the SDs. As shown in Fig. 3g and h, SD 1 seems to be most appropriate among the three SD-groups, as it leads to minor variations of the model parameter estimates over time, while preserving the adaptive properties of the estimator as shown in Fig. 3c. Unless specifically mentioned, SD 1 (the nominal SD group) is considered in the rest of the paper. The reader is also referred to Wang et al. (2007) for more results and interpretation in relation to the current test example.

3.2. A snowstorm case

This testing was conducted in the same A92 Freeway in 2004. The involved freeway stretch is displayed in Fig. 4. In fact, the stretch shown in Fig. 2a is the downstream part of this one (from the on-ramp with R4 to the downstream end). Note that the A92 Freeway was extended from a two-lane freeway either direction to a three-lane one in 2003 (with its detector configuration changed as well). Accordingly, the traffic flow characteristics may also have changed to an extent. It can be seen that five video detector stations (C2, C5, C6, C8, C10) and two loop detector stations (L1b and L2) are installed along the main stretch, while one loop detector station (L1a) is installed in a stretch merging into the main stretch, and two radar detector stations (R3 and R4) are installed respectively at the off-ramp and on-ramp. Fig. 5a and b display 24 h flow and speed measurements collected at C8, C6, and C2 on February 11, 2004. One may observe on the referred figures that the speed measurements decreased considerably from midnight until early morning, while the corresponding flow measurements kept steady at very low values. Surprisingly, the speed measurements during this time period were even lower than those during the afternoon peak period. Note that a similar observation was also delivered by the other detectors placed along the stretch on the same day. With the help of the local transportation authority, it was found out that a snowstorm was present in the area from the midnight until the morning of that day. It is not difficult to infer that the free speed along the test stretch decreased substantially under the snowstorm, which led to the observed speed decrease, despite a very low traffic flow.

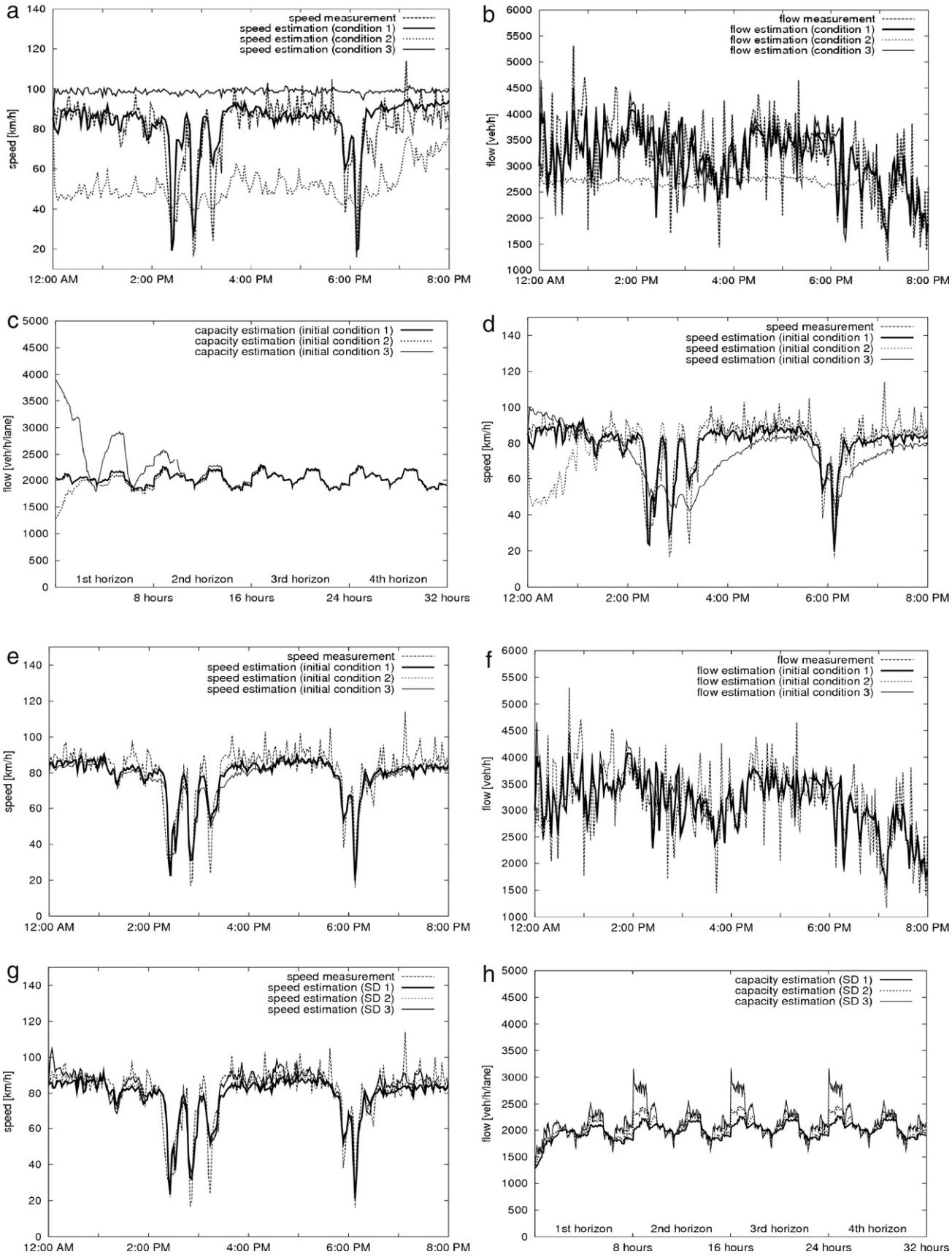

Fig. 3. A normal congestion case: (a) mean speed estimates at L2; (b) flow estimates at L2; (c) estimated capacity; (d) mean speed estimates at L2 (over the first time horizon); (e) mean speed estimates at L2 (over the second time horizon); (f) flow estimates at L2 (over the first time horizon); (g) mean speed estimates at L2 (over the third time horizon); (h) estimated capacity.

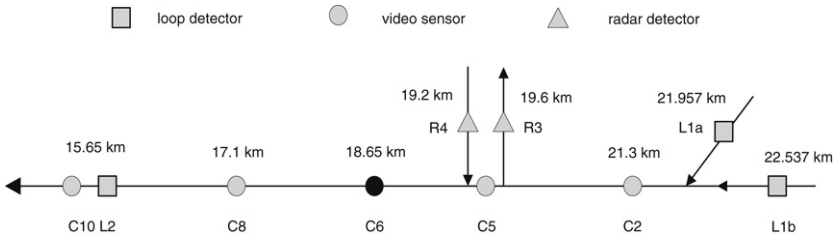

Fig. 4. Test stretch 2 in A92 freeway close to Munich: stretch layout and detector configuration.

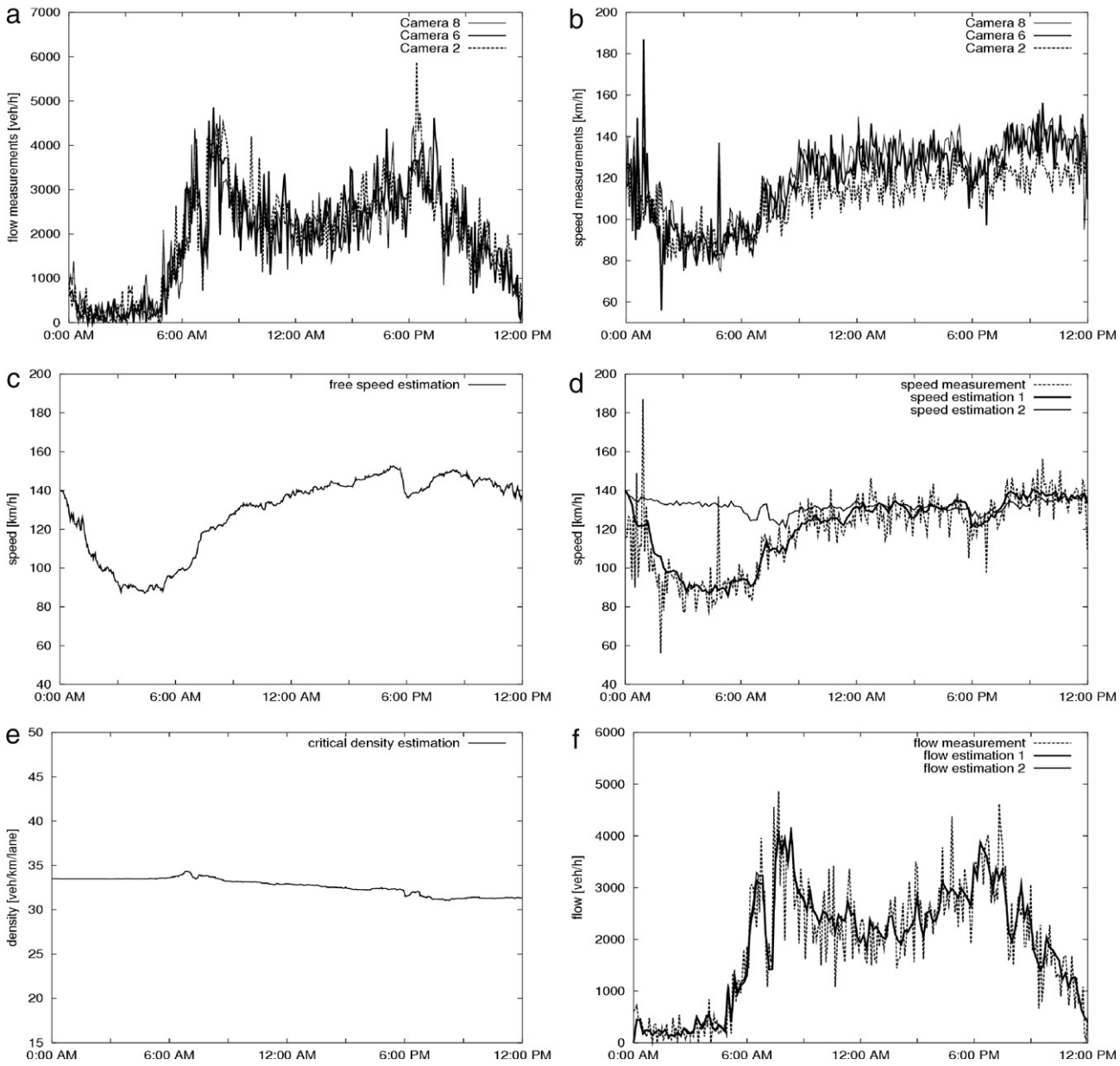

Fig. 5. A snowstorm case: (a) flow measurements; (b) mean speed measurements; (c) estimated free speed; (d) mean speed estimates at C6; (e) estimated critical density; (f) flow estimates at C6.

The designed traffic state estimator was ever tested in simulation with regard to an abrupt free speed drop (Wang & Papageorgiou, 2005). For the current real-data example, the test stretch is subdivided into a number of segments (each with a length of 280–600 m). For the sake of simplicity, the test stretch is assumed homogeneous in its traffic flow characteristics (i.e. assuming the same free speed, critical density, and capacity for the whole stretch), although this is actually not completely true at least for the free speed as it is visible in Fig. 5b. The utilized aggregated traffic measurement data was updated every minute while the time step of the estimator model was set equal to 5 s. The utilized **evaluation plan** is as follows: the flow and speed measurements at C2 and C8 as well as the flow measurements at R3 and R4 were fed to the estimator, while the flow and speed

measurements at C6 were used only for evaluating the estimation results. Typical testing results are presented in Fig. 5c–f. First, by activating the on-line model parameter estimation, the estimator is able to identify and track in real time the free speed decrease under the snowstorm (Fig. 5c) and deliver satisfactory speed estimates at C6 ("estimation 1" in Fig. 5d). It is noted that the on-line estimates of the critical density and exponent evolve steadily over time (see e.g. Fig. 5e for the critical density estimate); hence, in view of (7), the profile of the capacity estimation trajectory is very similar to that in Fig. 5c. Second, if the free speed is fixed at 140 km/h (i.e. forcing the estimator to ignore the snowstorm impact on the free speed), the estimator fails to track the speed decrease ("estimation 2" in Fig. 5d). However, in either case satisfactory flow estimates at C6 can be obtained (Fig. 5f) as the conservation equation (1) does not seem to be strongly impacted by the model mismatch.

Due to a strong fog from midnight until the morning of May 29, 2004, a speed limit of 80 km/h was applied in the A92 Freeway, which influenced the free speed and resulted in a clear speed decrease during the fog hours. Similarly good traffic state estimates were also obtained for that case (Wang, Papageorgiou, & Messmer, 2005).

3.3. An incident case

3.3.1. Traffic congestion types

From a traffic state estimation point of view, freeway traffic congestions can be classified as **normal** or **abnormal**. Given a freeway stretch, there are two types of normal congestions. Type 1 occurs within the freeway stretch due to overload, e.g. at an existing bottleneck, while Type 2 occurs sufficiently downstream of a considered stretch, creating an exogenous congestion shockwave that propagates upstream and may eventually spill back into the considered stretch. The normal congestions of Type 1 are typically recurrent congestions, while those of Type 2 may result from either recurrent congestions or traffic incidents. Under a normal congestion, the mean speeds upstream of the bottleneck (in the case of Type 1) or along the stretch (in the case of Type 2) gradually drop due to the shockwave propagation. For traffic state estimation under a normal congestion of Type 1, the macroscopic model employed by the estimator has sufficient knowledge regarding the existing bottleneck, so that the congestion may be well tracked by the estimator. A relevant simulation investigation was reported by Wang et al. (2003, 2006). In the case of a normal congestion of Type 2, an upstream-moving shockwave reaches the downstream boundary of the stretch and the speed and flow drops there are measured by the detectors installed at the boundary; thus, based on the utilized model, the estimator is able to predict the propagation of the shockwave inside the stretch. A relevant real-data testing was already presented in Section 3.1, where the congestion shockwave that was successfully tracked by the estimator, arrived indeed from the downstream of L3.

On the other hand, abnormal congestions are caused by traffic incidents (e.g. collisions, disabled cars, etc.), and are characterized by abrupt and substantial real-time changes of the impacted traffic flow characteristics, which may be reflected in corresponding changes of the model parameter values. When a traffic incident occurs within a freeway stretch, usually a non-recurrent bottleneck is created temporarily around the incident location, and the local capacity, free speed, and critical density decrease to an extent depending on the severity of the incident; moreover, the resulting congestion shockwave propagates upstream. It is noted that a same incident-incurred congestion can be an abnormal congestion for one stretch (if the incident occurs therein) but a normal congestion for another stretch (if the stretch is far upstream of the incident location). In addition, if an incident occurs outside of a freeway stretch but quite close to its downstream boundary, the resulting congestion may still have a clear impact on the local free speed, critical density, and capacity of that stretch.

Under an incident-incurred abnormal congestion, (a) a flow drop may be observed at the detectors downstream of the incident location, while the corresponding speed measurements may be seen to change only slightly; (b) both flow and speed drops may be observed at the detectors upstream of the incident location (if these detectors are not located too far upstream). Then, due to the contrast between the upstream and downstream measurements, the traffic state estimator is able to identify, via the on-line model parameter estimation, the occurrence of an abnormal event (of course, without knowing the exact reason). A real-data testing under an abnormal congestion is reported below.

3.3.2. Incident alarm

This test was conducted in the same stretch as shown in Fig. 4, using the same evaluation plan as for the snowstorm case. Fig. 6a and b display the flow and speed measurements collected on April 18, 2004. (Notice that the speed measurements are around 130 km/h from midnight until early morning, in contrast to those shown in Fig. 5b under the snowstorm.) One may observe from Fig. 6c and d that:

- During 7:15 PM–7:40 PM, the flow trajectories drop to the range of 0–500 veh/h in the sequence C10–C8–C6–C5.
- During 6:30 PM–8:10 PM, the speed trajectories drop to less than 25 km/h in the sequence C8–C6–C5, and recover later in the opposite sequence.
- An abrupt speed drop is observed at C8 during 6:30 PM–8:10 PM, while no speed drop is observed at C10; on the other hand, the flow measurements at C8 and C10 drop almost simultaneously at about 7:15 PM and recover after 7:40 PM.
- No obvious speed or flow drop is observed at C2.

These observations indicate that an incident (or abnormal event) occurred between C10 and C8, which gave rise to a capacity drop in the stretch including C8, C6, and C5 and led to a sharp abnormal congestion shockwave propagating upstream, albeit without ever reaching C2 (because many drivers chose to escape the freeway via the off-ramp with R3 during the congestion, as confirmed with the R3 flow measurements).

Some representative testing results are presented in Fig. 6e–h. During the incident period, both sharp critical density drop and capacity drop are identified in real-time (Fig. 6e and f). The comparison between Figs. 6f and 3c (the third time horizon) indicates that the respective traffic situations are quite different. To further highlight the abrupt capacity variation due to the incident, Fig. 6g and h contrast the time-derivative of the estimated capacity in both cases. In fact, the on-line parameter estimation in Fig. 6e and f delivered the first indication on the existence of the incident, upon which the presented data analysis was conducted to confirm the incident presence. The flows and mean speeds are estimated fairly well with on-line model parameter estimation; see trajectories "estimation 1" in Fig. 7 for the flow and speed estimates at C6. With fixed model parameter values, however, a speed estimation bias is created (trajectories "estimation 2"), under free-flow conditions.

It is also noticed in Fig. 6e and f that, after the abrupt parameter drops due to the incident, the model parameter estimates did not recover promptly, although this has no impact on the flow and speed estimates (Fig. 7). This is because the traffic flow was under a lasting (night) free-flow condition after the incident (see Fig. 6a and b), in which case the traffic measurements (illustrated by the dots in Fig. 1) do not contain sufficient information in relation to the critical density and capacity. An extended investigation has

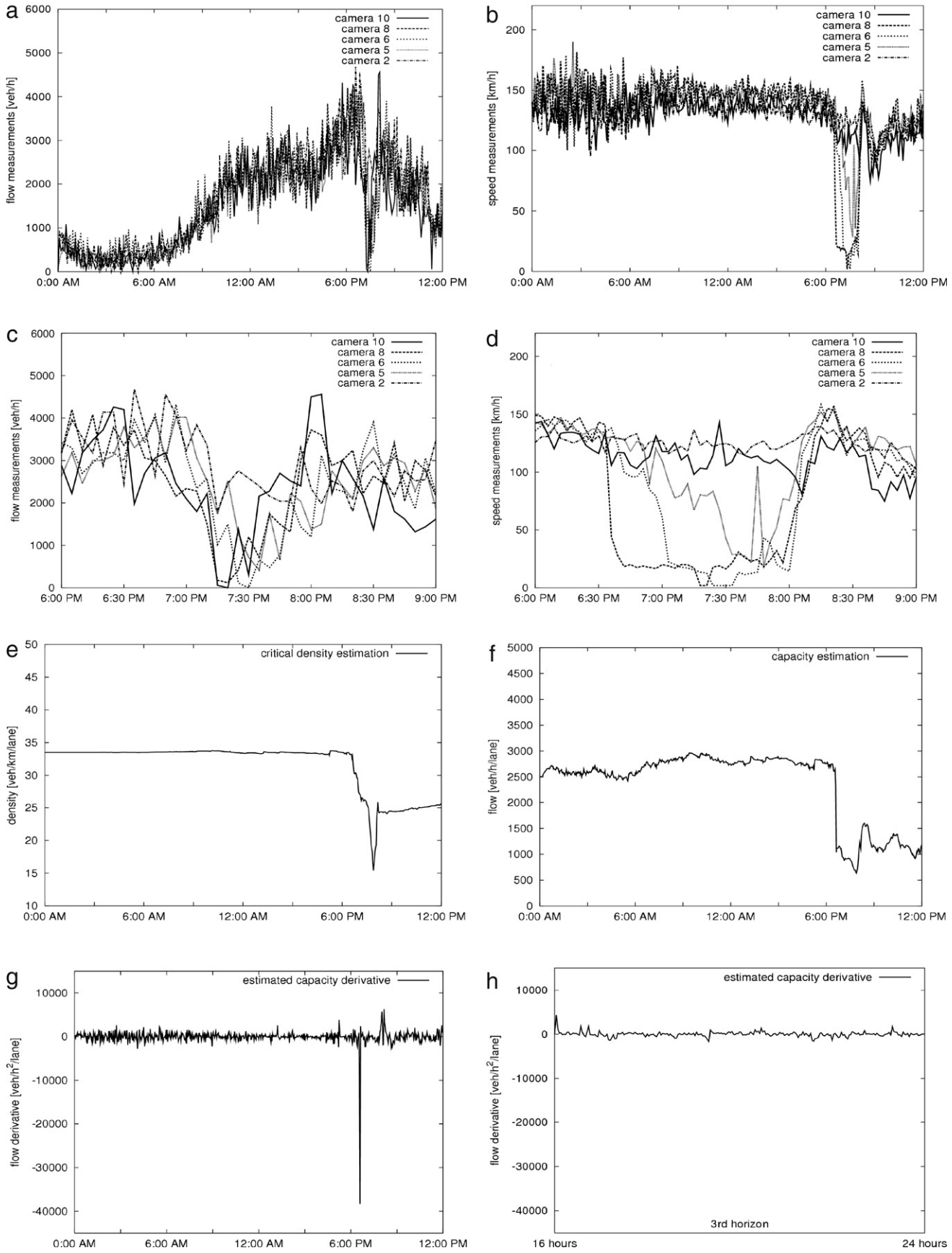

Fig. 6. An incident case: (a) flow measurements; (b) mean speed measurements; (c) zoom on the flow-drop period in (a); (d) zoom on the speed-drop period in (b); (e) estimated critical density; (f) estimated capacity; (g) and (h) estimated capacity derivative.

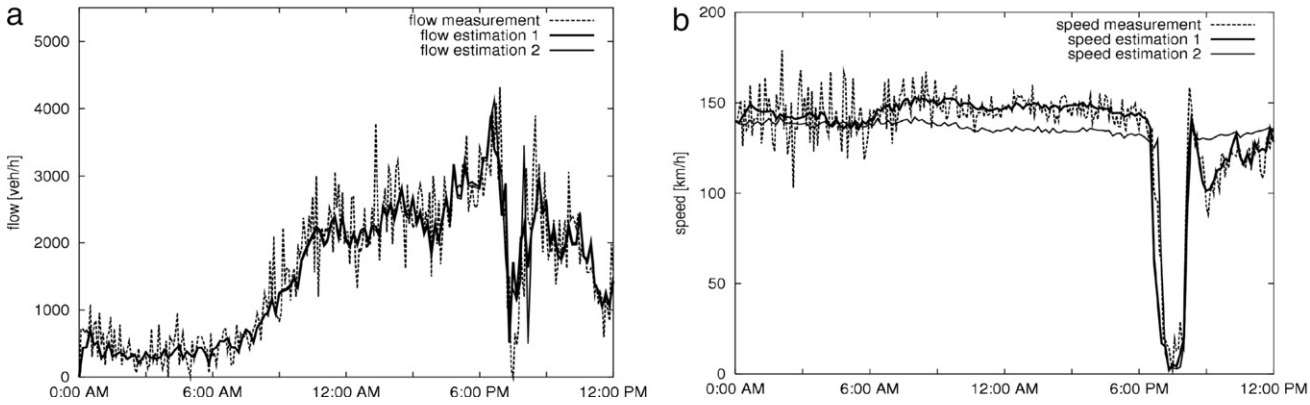

Fig. 7. An incident case: (a) flow estimates at C6; (b) mean speed estimates at C6.

shown that the parameter estimates recover from the drops in the next day, soon after the traffic flow assumes considerably higher values than during the night. This underlines that, in order to identify well all model parameters, the estimator needs to be persistently excited with traffic measurement data covering a sufficiently large spectrum of possible traffic flow conditions.

4. A large-scale field application

Recently the real-time freeway network traffic surveillance tool RENAISSANCE has been developed (Wang et al., 2006), which bases its various traffic surveillance functions upon the presented traffic state estimator. Since April 2006, RENAISSANCE has been operational in the South-Italian freeway traffic control center in Naples to supervise the A3 Freeway. The A3 Freeway has a total directed length of about 100 km and connects the municipalities of the coastal strip along the southern slope of Mount Vesuvius with Naples and Salerno (Fig. 8a). Freeway A3 actually serves one of the most congested metropolitan areas in southern Italy. Fig. 8b presents a schematic diagram of the A3 layout in both Naples and Salerno directions. The A3 detector configuration is also presented in Fig. 8b, where each black dot represents a video detector that offers both flow and speed measurements, and each black triangle just upstream of each pair of on-ramps represents a toll station that records only the number of passing vehicles. The measurement interval is irregular but of 30 s on average while the model time step is set equal to 5 s. The detectors are rather sparsely installed in the freeway mainstream, with an average spacing of 4 km within the first 20 km and of about 7 km within the next 27.5 km.

From the modeling point of view, this test site, including a number of internal bifurcations at the immediate downstream of some toll stations, has to be modeled as a freeway network. In other words, both directions of A3 must be considered all together, else the partial missing of independent on-ramp and off-ramp measurements would damage the observability of the corresponding traffic dynamic system and thus render infeasible the state estimation task and further traffic surveillance tasks. Significant spatial difference may daily be observed from mainstream speed measurements under free-flow conditions (see e.g. Fig. 9a for speed measurements collected in the Naples direction). This indicates traffic flow inhomogeneity; in other words, the free speed value may change over a long freeway stretch due to the involved curvature, upgrade, tunnels, etc. To address such traffic flow inhomogeneity, multiple fundamental diagrams were introduced to the estimator model, each like the one shown in Fig. 1, addressing a directional stretch between two mainstream detectors. In this context, the on-line model parameter estimation refers to joint estimation of multiple fundamental diagram parameters and normal traffic flow variables, still under the presented modeling and EKF framework. For the A3 test example, 17 fundamental diagrams and totally 516 state variables were involved, 80 of which were measured. In fact, it is the first time to report on the real-time field application of traffic state estimation to so large a freeway site.

A test was conducted with measurement data collected from A3 on October 9, 2006. In addition to the traffic flow inhomogeneity displayed in Fig. 9a, 9b shows that D10025 in the Salerno direction broke down from 12:00 PM onward during the day (see also the corresponding flow measurements in Fig. 11b or f). Fed with these measurements, the estimator delivers speed and flow estimates with a spatial resolution of 500 m. First, some representative speed estimation results at some detector locations in the Naples-bound direction are presented in Fig. 10 along with the free speed estimates for the sections downstream bounded by those detectors. Clearly, the traffic flow inhomogeneity is well identified via the free speed estimates. A speed decrease between 6:00 PM and midnight was recorded by D10024 (Fig. 10c), while the corresponding flow measurements are rather low (the figure omitted). Similar to the snowstorm case presented in Section 3.2, this indicates the occurrence of a certain abnormal event leading to the decrease of free speed, which is also confirmed by the local free speed estimation (Fig. 10d). Second, as indicated by Fig. 9b, this test example also offers a chance to observe the impact of a disabled detector on the traffic state estimation performance. Without any mechanism for detector fault alarms, the faulty measurements were considered by the estimator as reflecting the ground truth. Consequently, a huge fictitious congestion was created at D10025 in the estimator model, which propagated upstream until Naples for the rest of the day (Fig. 11a and b). Meanwhile drastic drops of the free speed and capacity resulted in the estimator model only for the freeway section upstream of D10025 (Fig. 11c and d), in order for the model output to be in agreement with the faulty measurements. However, if the measurements of D10025 would not be fed to the estimator, then the faulty impact of D10025 does not appear in the estimation results (see Fig. 11e and f), while the local model parameter estimates look normal (Fig. 11g and h). This interesting test example suggests that:

- The on-line model parameter estimation may also be used as an indicator for real-time detector faults if this information is not directly provided by traffic detectors or via another method;
- If a reliable mechanism for detector fault alarm is available, the estimator would be able to avoid the impact of faulty measurements on traffic state estimation via real-time self-reconfiguration (e.g. by excluding the faulty measurements from (17), provided that this does not violate flow observability).

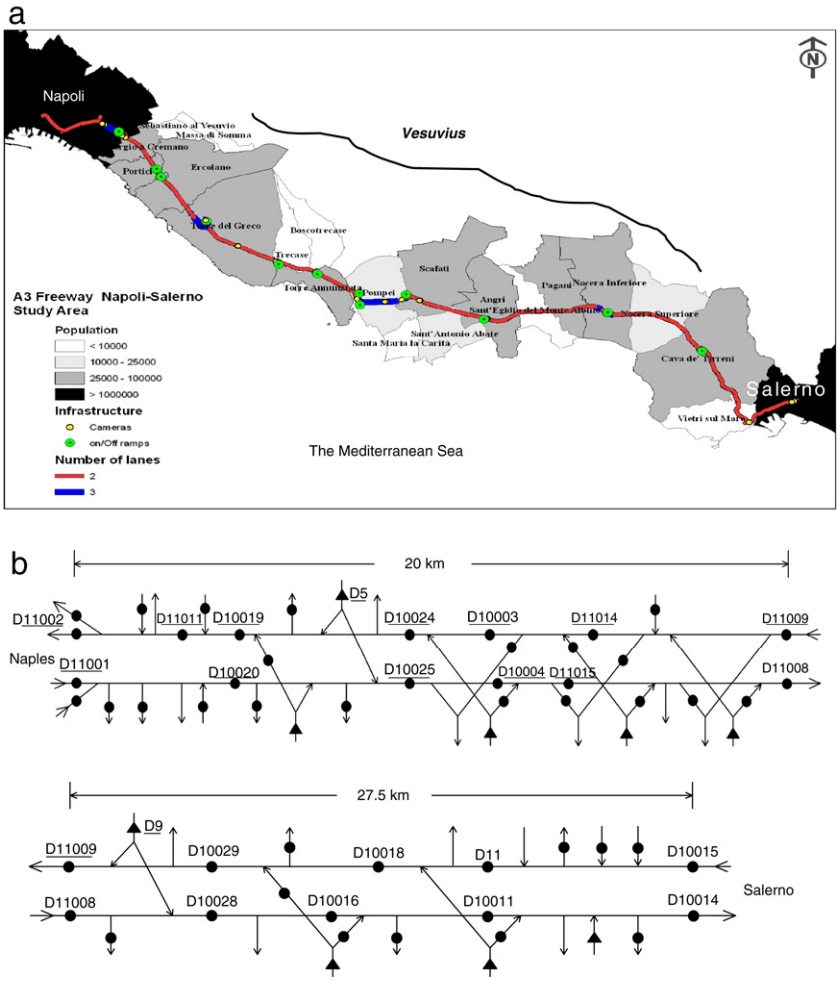

Fig. 8. The A3 freeway between Naples and Salerno in south Italy: (a) geographical illustration of A3; (b) A3 layout and detector configuration (with each dot representing a video sensor and each triangle representing a toll station).

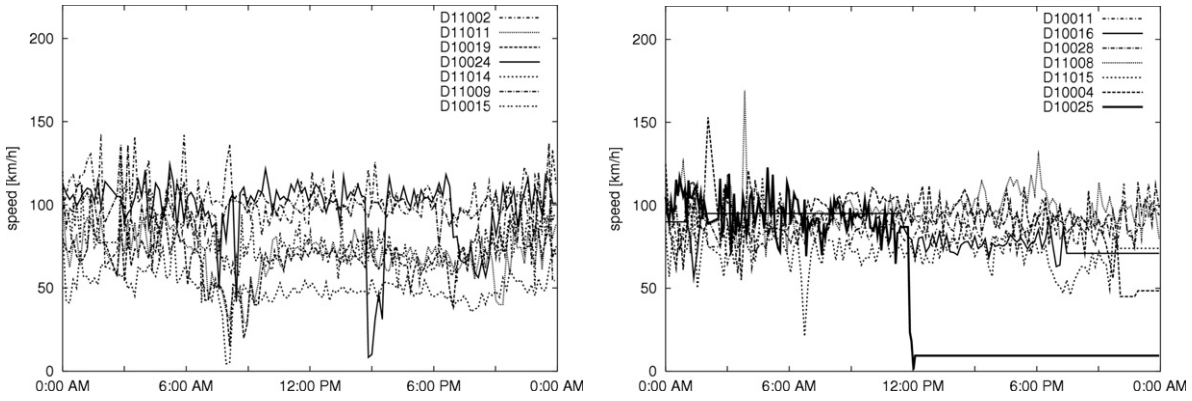

(a) In the Naples direction.

(b) In the Salerno direction.

Fig. 9. Speed measurements along the A3 freeway on October 9, 2006.

In summary, this large-scale application example provides a platform for an overall testing of the traffic state estimator in case of sparse measurement availability, spatial traffic flow inhomogeneity, abnormal events, detector faults, general measurement inaccuracy, etc. Further field installations of RENAISSANCE are currently in progress in various countries.

5. Conclusive remarks

A number of real-data tests have been reported in this paper to evaluate the performance of a generic freeway traffic state estimator under various traffic situations. The testing results demonstrate that, as compared to the traffic state estimators developed in the past, this estimator has four distinguished features enabled with joint state and parameter estimation. The first feature is that the estimator is able to work satisfactorily without a prior need for off-line model calibration. More specifically,

- The on-line model parameter estimation is indispensable for proper traffic state estimation, particularly in case of poor prior model calibration.
- The estimator with the on-line model parameter estimation is able to deliver satisfactory traffic state estimates under

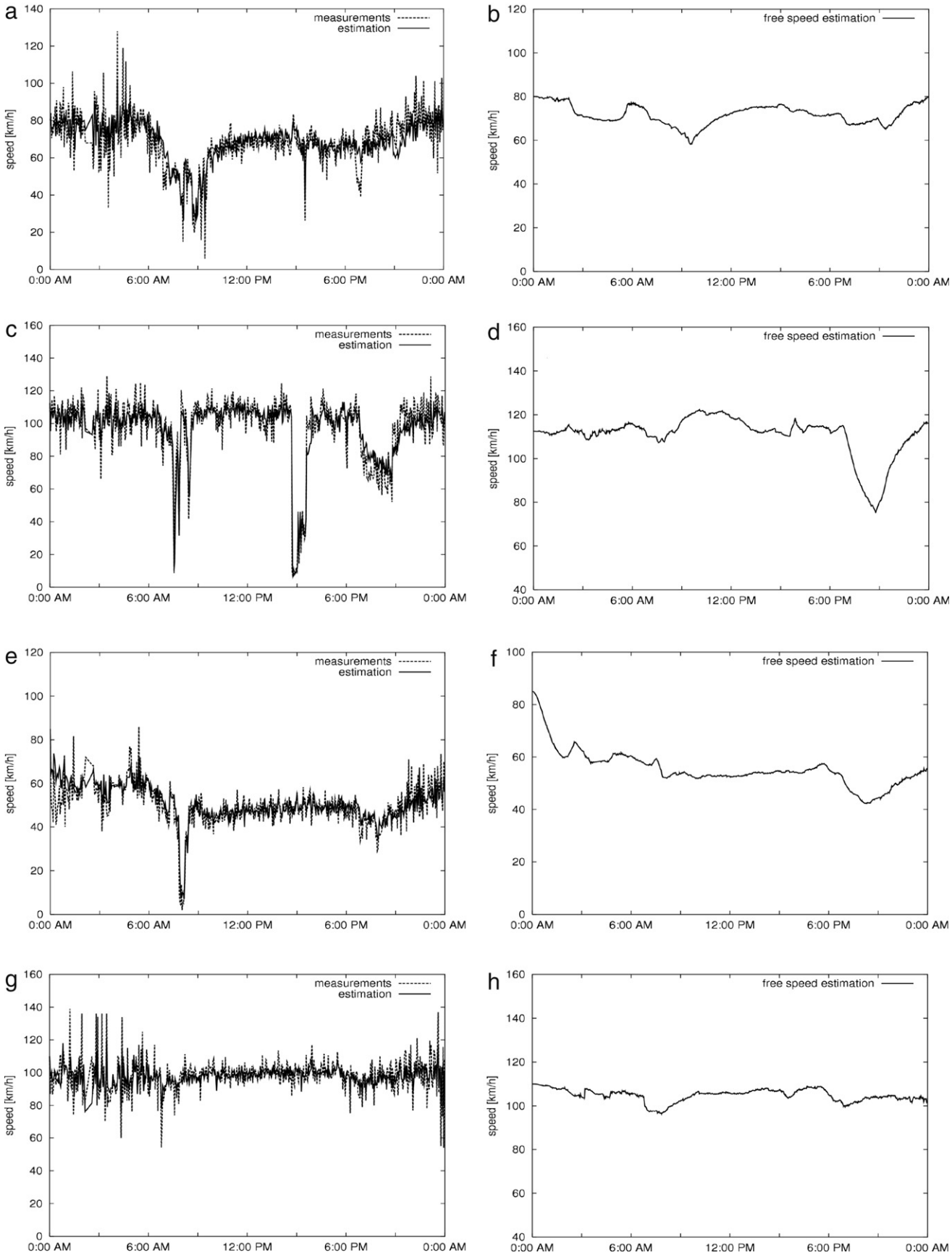

Fig. 10. Traffic state estimation results in A3: (a) and (b) speed and free speed estimates around D10019; (c) and (d) speed and free speed estimates around D10024; (e) and (f) speed and free speed estimates around D11014; (g) and (h) speed and free speed estimates around D11009.

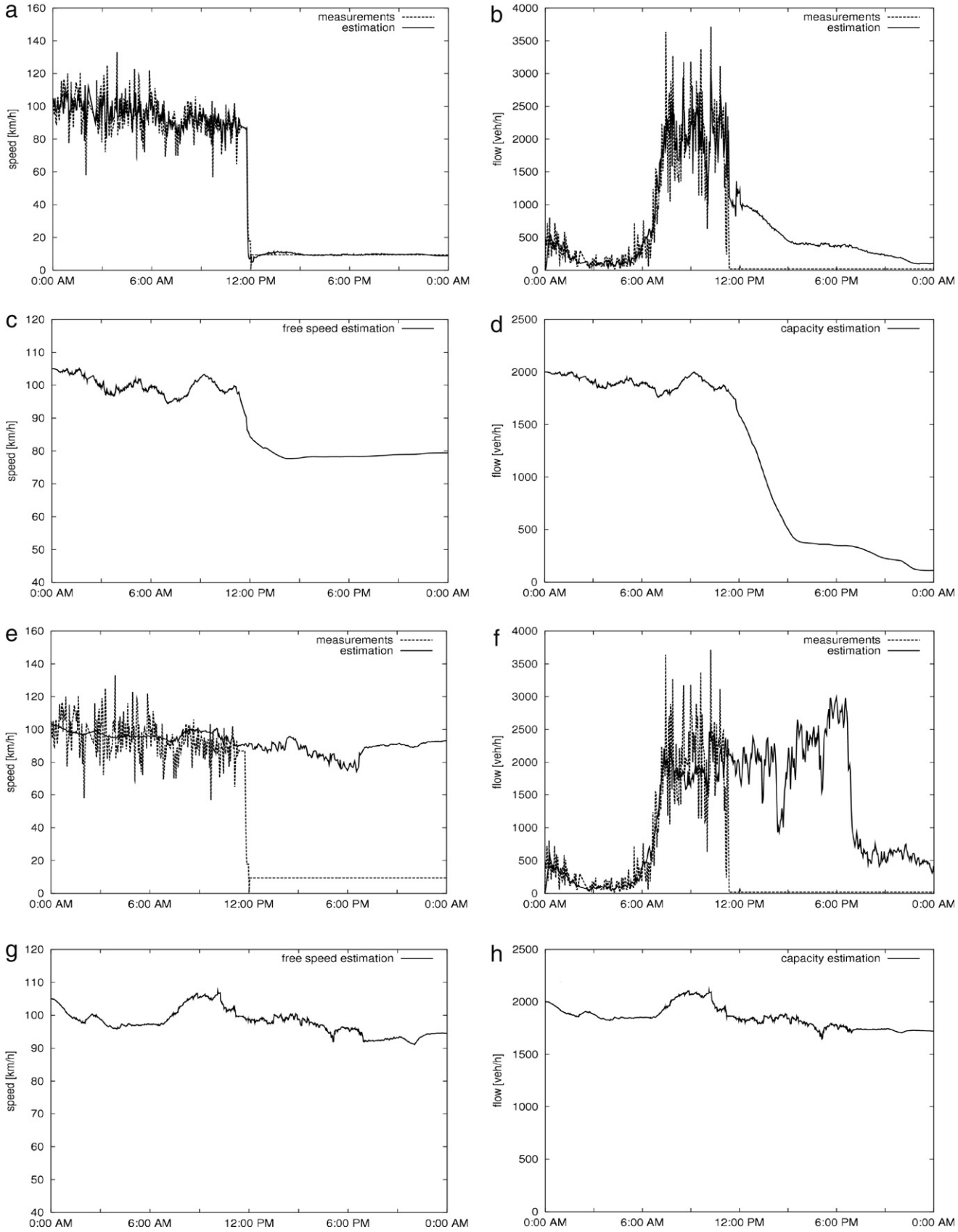

Fig. 11. Detector fault alarm: (a)–(d) using the faulty measurements from D10025; (e)–(h) without using the faulty measurements from D10025.

various traffic conditions (fluid, dense, congested), despite a large average inter-detector spacing (4–7 km).
- The estimator is little sensitive to the initial values of the model parameters and traffic flow variables as well as to the related standard deviations.

The second feature is that the estimator can adapt itself efficiently to the changes of weather conditions (like snow, fog, etc.), traffic composition (percentage of trucks), and control measures (e.g. variable speed limits applied). The third feature is that under an incident-incurred abnormal congestion the estimator is able to issue an incident alarm promptly, while handling the traffic state estimation adequately. The fourth feature is that the estimator is capable of issuing alarms regarding obvious detector faults. The real-time freeway network traffic surveillance tool RENAISSANCE (Wang et al., 2003, 2006) developed on the basis of the reported adaptive traffic state estimator has been operational in the Naples freeway traffic control center in south Italy since April 2006 (Wang et al., in press), and will be soon implemented in the Antwerp freeway traffic control center in Belgium and further freeway networks.

The state estimation of nonlinear systems corrupted with noise has been extensively considered in research and applications. Because the optimal solution to this problem is infinite dimensional (see e.g. Kushner (1967)), a variety of approximate (or suboptimal) approaches have been developed, among which the extended Kalman filter (EKF) is probably most widely used (see e.g. Jazwinsky (1970) and Sorenson (1985)). In the past three decades, numerous successful applications of the EKF have been reported in the literature, but some intractable difficulties have also been encountered. For example, the use of EKF was reported in some applications to lead to biased estimates or even divergence, due to stepwise linearization (Julier & Uhlmann, 2004; Norgaard, Poulsen, & Ravn, 2000; Romanenko & Castro, 2004), inappropriate initial state estimates (Glielmo, Setola, & Vasca, 1999; Ljung, 1979; Reif, Sonnemann, & Unbehauen, 1998), unknown covariance matrices of involved noise, or even the Gaussianity assumption of involved noise (Arulampalam, Maskell, Gordon, & Clapp, 2002; Chen, Morris, & Martin, 2005), etc. To address such problems, some other nonlinear filtering methods, especially unscented Kalman filtering (UKF) (Julier & Uhlmann, 2004) and particle filtering (PF) (Arulampalam et al., 2002), have been tested for a variety of state estimation applications, gaining increasing popularity. Recently such attempts towards traffic state estimation have also appeared (Antoniou, Ben-Akiva, & Koutsopoulos, 2007; Hegyi, Girimonte, Babuska, & De Schutter, 2006; Mihaylova, Boel, & Hegyi, 2007).

The reported results demonstrate that the application of the EKF to traffic state estimation is not strongly affected by the above-mentioned difficulties. In addition to the estimator's adaptive features shown, the estimator is seen little sensitive to the involved noise statistics. More precisely, satisfactory functioning of the traffic state estimator does not seem to require a prior knowledge of noise characteristics (distribution or mean/covariance), and this facilitates general applicability of the estimator. Nevertheless, comparable evaluations of EKF with UKF and PF for this significant application problem could indicate accuracy advantages of one or another filtering approach.

Besides accuracy, adaptiveness, and robustness, another concern regarding traffic state estimation in relation to practical applications is the computational real-time properties. In this aspect the EKF-based approach is clearly superior to the UKF-based or PF-based methods. For instance, the presented EKF-estimator took 11 h 34 min in a Pentium 4 personal computer (2.80 GHz, 1 GB RAM, Windows XP) to deal with 24 h measurement data (with a measurement updating interval of 30 s to 1 min on average) from the whole A3 network with a total directed length of some 100 km. On the other hand, approaches may also be sought to improve the computational cost-effectiveness of alternative filtering methods (see e.g. Hegyi, Mihaylova, and Boel (2007)).

Acknowledgements

This research was partly supported by the European Commission's IST (Information Society Technologies) Program under the project RHYTHM (IST-2000-29427). The authors thank Mr. O. Ernhofer and Mr. Th. Heinrich from TRANSVER GmbH (Munich, Germany) for providing the utilized real traffic measurement data from the A92 Freeway close to Munich, Germany. The application of RENAISSANCE to the A3 Freeway in southern Italy was partly supported by the Italian Ministry of University and Research under the project PON-SAM (No. 12897). The authors wish to thank the project manager Mr. Luigi Massa from SAM (Società Autostrade Meridionali) in Naples, Italy. The completion of this paper was also supported in part by the Engineering New Staff Member Research Fund and Engineering Small Grant (2008), Monash University, Australia. All statements of this paper are under the sole responsibility of the authors and do not necessarily reflect the European Commission's, the Italian Ministry of University and Research's, Monash University's, or other partners' policies or views. This paper was partially presented at the 2005 IEEE Conference on Intelligent Transportation Systems and the 2006 Transportation Research Board Annual Meeting. The authors wish to thank anonymous reviewers for their critically helpful comments on a previous version of the paper; in particular, the authors are much grateful to one reviewer and the associate editor for their constructive suggestion that led to the adding of the large-scale field test example.

References

Antoniou, C., Ben-Akiva, M., & Koutsopoulos, H. N. (2007). Nonlinear Kalman filtering algorithms for on-line calibration of dynamic traffic assignment models. *IEEE Transactions on Intelligent Transportation Systems*, *8*, 661–670.

Arulampalam, M. S., Maskell, S., Gordon, N., & Clapp, T. (2002). A tutorial on particle filters for online nonlinear/non-Gaussian Bayesian tracking. *IEEE Transactions on Signal Processing*, *50*, 174–188.

Chen, T., Morris, J., & Martin, E. (2005). Particle filters for state and parameter estimation in batch processes. *Journal of Process Control*, *15*, 665–673.

Cremer, M., & Papageorgiou, M. (1981). Parameter identification for a traffic flow model. *Automatica*, *17*, 837–843.

Glielmo, L., Setola, R., & Vasca, F. (1999). An interlaced extended Kalman filter. *IEEE Transactions on Automatic Control*, *44*, 1546–1549.

Hegyi, A., Girimonte, D., Babuska, R., & De Schutter, B. (2006). A comparison of filter configurations for freeway traffic state estimation. In *Proceedings of the 9th international IEEE conference on intelligent transportation systems*.

Hegyi, A., Mihaylova, L., & Boel, R. (2007). Parallelized particle filtering for freeway traffic state tracking. In *Proceedings of the 2007 European control conference*.

Jazwinsky, A. H. (1970). *Stochastic processes and filtering theory*. New York: Academic Press.

Julier, S. J., & Uhlmann, J. K. (2004). Unscented filtering and nonlinear estimation. *Proceedings of IEEE*, *92*, 401–422.

Kyte, M., Khatib, Z., Shannon, P., & Kitchener, F. (2001). The effect of weather on free flow speed. In *Proceedings (CD-ROM) of transportation research board 80th annual meeting*. Paper No. 01-3280.

Kushner, H. J. (1967). Dynamical equations for optimum non-linear filtering. *Journal of Differential Equations*, *3*, 179–190.

Ljung, L. (1979). Asymptotic behavior of the extended Kalman filter as a parameter estimator for linear systems. *IEEE Transactions on Automatic Control*, *24*, 36–50.

Mihaylova, L., Boel, R., & Hegyi, A. (2007). Freeway traffic estimation within particle filtering framework. *Automatica*, *43*, 290–300.

Norgaard, M., Poulsen, N. K., & Ravn, O. (2000). New developments in state estimation for nonlinear systems. *Automatica*, *36*, 1627–1638.

Papageorgiou, M., Blosseville, J.-M., & Haj-Salem, H. (1990). Modelling and real-time control of traffic flow on the southern part of Boulevard Périphérique in Paris-Part I: Modelling. *Transportation Research A*, *24*, 345–359.

Papageorgiou, M., Kosmatopoulos, E., & Papamichail, I. (2008). Effects of variable speed limits on motorway traffic flow. In *Proceedings (CD-ROM) of the 87th transportation research board meeting*. Paper Number: 08-0781.

Papamichail, I., Papageorgiou, M., & Wang, Y. (2007). Motorway traffic surveillance and control. *European Journal of Control*, *13*, 297–319.

Reif, K., Sonnemann, F., & Unbehauen, R. (1998). An EKF-based nonlinear observer with a prescribed degree of stability. *Automatica*, *34*, 1119–1123.

Romanenko, A., & Castro, J. A. (2004). The unscented filter as an alternative to the EKF for nonlinear state estimation: A simulation case study. *Computers and Chemical Engineering*, *28*, 347–355.

Sorenson, H. W. (1985). *Kalman filtering: Theory and application*. New York: IEEE Press.

Wang, Y., Papageorgiou, M., & Messmer, A. 2003. Algorithms and preliminary testing for traffic surveillance. *Deliverable 3.2 for the Project RHYTHM (IST-2000-29427)*, report for the Information Society Technologies Office of the European Commission. Brussels, Belgium.

Wang, Y., & Papageorgiou, M. (2005). Real-time freeway traffic state estimation based on extended Kalman filter: A general approach. *Transportation Research B*, *39*, 141–167.

Wang, Y., Papageorgiou, M., & Messmer, A. 2005. An adaptive freeway traffic state estimator and its real data testing, Part II: Adaptive capabilities. In *Proceedings of IEEE 8th international conference on intelligent transportation systems* (pp. 537–542).

Wang, Y., Papageorgiou, M., & Messmer, A. (2006). RENAISSANCE — a unified macroscopic model based approach to real-time freeway network traffic surveillance. *Transportation Research C*, *14*, 190–212.

Wang, Y., Papageorgiou, M, & Messmer, A. (2007). Real-time freeway traffic state estimation based on extended Kalman filter: A case study. *Transportation Science*, *41*, 167–181.

Wang, Y., Coppola, P., Messmer, A., Tzimitsi, A., Papageorgiou, M., & Nuzzolo, A. (2008). Real-time freeway network traffic surveillance: Large-scale field testing results in southern Italy. *IEEE Transactions on Intelligent Transportation Systems* (in press).

Yibing Wang received the B.Sc. degree in Electronics and Computer Engineering from Sichuan University, China, the M. Eng. degree in Automatic Control Engineering from Chongqing University, China, and the Ph.D. degree in Control Theory and Applications from Tsinghua University, China. He was with the Dynamic Systems and Simulation Laboratory, Department of Production Engineering and Management, Technical University of Crete, Greece, where he was a Postdoctoral Researcher from 1999 to 2001 and a Senior Research Fellow from 2001 to 2007. He is currently a Senior Lecturer with the Department of Civil Engineering, Monash University, Melbourne, Australia. His research interests include traffic flow modelling, freeway traffic surveillance, ramp metering, route guidance, urban traffic signal control, vehicular infrastructure integration. He has published more than 20 international journal papers and book chapters. He has extensive research and development experience on intelligent transportation systems (ITS). From 2000 to 2007, he participated in several European projects on ITS and collaborated with transportation research and practice professionals from Greece, Germany, UK, Belgium, Italy, and The Netherlands. Dr. Wang is a member of IEEE, an Associate Editor for the IEEE Transactions on Intelligent Transportation Systems, the Book Review Editor of Transportation Research Part C: Emerging Technologies, an Associate Editor for the International Journal of Vehicle Information and Communication Systems, an Editorial Board Member of The Open Transportation Journal. He was a vice chair of the International Program Committee of the 9th IEEE Annual Conference on Intelligent Transportation Systems (Toronto, 2006).

Markos Papageorgiou was born in Thessaloniki, Greece, in 1953. He received the Diplom-Ingenieur and Doktor-Ingenieur (honors) degrees in Electrical Engineering from the Technical University of Munich, Germany, in 1976 and 1981, respectively. From 1976 to 1982 he was a Research and Teaching Assistant at the Control Engineering Chair, Technical University of Munich. He was a Free Associate with Dorsch Consult, Munich (1982–1988), and with Institute National de Recherche sur les Transports et leur Sécurité (INRETS), Arcueil, France (1986–1988). From 1988 to 1994 he was a Professor of Automation at the Technical University of Munich. Since 1994 he has been a Professor at the Technical University of Crete, Chania, Greece. He was a Visiting Professor at the Politecnico di Milano, Italy (1982), at the Ecole Nationale des Ponts et Chaussées, Paris (1985–1987), and at MIT, Cambridge (1997, 2000); and a Visiting Scholar at the University of Minnesota (1991, 1993), the University of Southern California (1993) and the University of California, Berkeley (1993, 1997, 2000).

Dr. Papageorgiou is the author of the books *Applications of Automatic Control Concepts to Traffic Flow Modeling and Control* (Springer, 1983) and *Optimierung* (Oldenbourg, 1991; 1996), the editor of the *Concise Encyclopedia of Traffic and Transportation Systems* (Pergamon Press, 1991), and co-author of *Optimal Real-time Control of Sewer Networks* (Springer, 2005) and the author or co-author of some 300 technical papers. His research interests include automatic control and optimization theory and applications to traffic and transportation systems, water systems and further areas. He is the Editor-in-Chief of *Transportation Research — Part C* and an Associate Editor of *IEEE Control Systems Society — Conference Editorial Board*. He also served as an Associate Editor of *IEEE Transactions on Intelligent Transportation Systems* and other journals. He was Chairman (1999–2005) and Vice-Chairman (1994–1999) of the IFAC Technical Committee on Transportation Systems. He is a Fellow of IEEE. He received a DAAD scholarship (1971–1976), the 1983 Eugen–Hartmann award from the Union of German Engineers (VDI), and a Fulbright Lecturing/Research Award (1997). He was the (first) recipient (2007) of the IEEE Outstanding ITS Research Award.

Albert Messmer received the Diplom-Ingenieur and Doktor-Ingenieur degrees in Electrical Engineering (with a focus on control engineering) from the Technical University of Munich, Germany, in 1983 and 1994, respectively. Since 1994 he has been working as an independent consultant. Since 1983 he has been engaged in modelling, simulation, optimization, and control of motorway networks and sewer systems. He has written more than 30 technical papers on modelling and control of water flow and freeway traffic.

Dr. Messmer is a member of the Union of German Engineers (VDI).

Pierluigi Coppola, born in Naples (Italy) in 1972, received the M. Eng. degree in Civil Engineering and the Ph.D. in Road Infrastructures and Transportation Systems from the "Federico II" University of Naples. He is currently an assistant professor in Transportation planning at the Faculty of Engineering of "Tor Vergata" University of Rome. His research interests include Advanced Travellers Information Systems (ATIS) for road networks and Public Transportation systems, Land-Use/Transport Interactions (LUTI) models and network design methods. He has published 30 journal papers and book chapters. From 1998 to 2007 he has been involved in European and National research projects and practice professional on travel demand forecasting, network design and ITS, in Italy and in The Netherlands. Dr Coppola is a member of the Program Committee of the European Transport Conference (ETC).

Athina Tzimitsi was born in Naoussa, Greece, in 1974. She received the Diploma of Production Engineering and Management and Master of Operational Research from Technical University of Crete, Greece, in 2005 and 2007, respectively. She was with the Dynamic Systems and Simulation Laboratory at Technical University of Crete from 2004 to 2008. She is now working in the private sector.

Agostino Nuzzolo, born in Calvi (Italy) in 1949, is a full professor of Transportation Planning at the Faculty of Engineering of "Tor Vergata" University of Rome. His research work is relative to the field of the theory of transportation systems and its application in transportation analysis, modeling and planning. He is the author or co-author of four books on the schedule-based approach to dynamic transportation networks and some 150 technical papers and book chapters. Prof. Nuzzolo is currently the president of the Italian Society of Lecturers of Transports (SIDT). He has been responsible of National and International research projects on Traffic and Transportation Planning, Railway Services Pricing and Design, Master Transport Plans, and on technical-economic feasibility studies of transport infrastructures.